Díaz Isabel (Orcid ID: 0000-0001-9865-902X)
Romero-Puertas Maria (Orcid ID: 0000-0002-4854-896X)
Olmedilla Adela (Orcid ID: 0000-0002-8556-3739)
Sandalio Luisa (Orcid ID: 0000-0002-8550-7577)

Cadmium induces ROS-dependent pexophagy in Arabidopsis leaves

Nieves Calero-Muñoz[1*], Marino Exposito-Rodriguez [2], Aurelio M. Collado-Arenal[1], María Rodríguez-Serrano M.[11], Ana M. Laureano-Marín[3], M. Estrella Santamaría [4], Cecilia Gotor[3], Isabel Díaz[4], Philip M. Mullineaux [2], María C. Romero-Puertas[1], Adela Olmedilla[1], Luisa M. Sandalio[1]

1 Department of Biochemistry and Molecular and Cellular Biology of Plants, Estación Experimental del Zaidín, CSIC, 18008 Granada, Spain.

2 School of Biological Sciences, University of Essex, Wivenhoe Park, Colchester CO4 3SQ

3 Institute of Plant Biochemistry and Photosynthesis, CSIC and Universidad de Sevilla, 41092 Spain.

4 Centre for Plant Biotechnology and Genomics, Universidad Politécnica de Madrid (UPM), The National Institute for Agricultural and Food Research and Technology (INIA), Campus Montegancedo, 28223 Pozuelo de Alarcón, Madrid, Spain

1*Current address: Centre of Molecular Biology Severo Ochoa, CSIC, Madrid, Spain

11 Current address: Faculty of Education, University of Granada, Melilla, Spain

Correspondence:

LM Sandalio, Department of Biochemistry and Cellular and Molecular Biology of Plants, Estación Experimental del Zaidín, CSIC, 18008 Granada, Spain.

E-mail: luisamaria.sandalio@eez.csic.es

Abstract

Cadmium treatment induces transient peroxisome proliferation in Arabidopsis leaves. To determine whether this process is regulated by pexophagy and to identify the mechanisms involved, we analyzed time course-dependent changes in ATG8, an autophagy marker, as well as the accumulation of peroxisomal marker PEX14a. After 3 h of Cd exposure, the transcript levels of *ATG8h, ATG8c, a* and *i,* were slightly up-regulated and then returned to normal. ATG8 protein levels also increased after 3 h of Cd treatment, while an opposite pattern was observed in PEX14. Arabidopsis lines expressing GFP-ATG8a and CFP-SKL enabled us to demonstrate the presence of pexophagic processes in leaves. The Cd-dependent induction of pexophagy was demonstrated by the accumulation of peroxisomes in autophagy (ATG)-related Arabidopsis knockout mutants *atg5 and atg7*. We show that ATG8a co-localizes with catalase and NBR1 in the electron-dense peroxisomal core, thus suggesting that NBR1 may be an autophagic receptor for peroxisomes, with catalase being possibly involved in targeting pexophagy. Protein carbonylation and peroxisomal redox state suggest that protein oxidation may trigger pexophagy. Cathepsine B, legumain and caspase 6 may also be involved in the regulation of pexophagy. Our results suggest that pexophagy could be an important step in rapid cell responses to cadmium.

Key words: ATG8, cadmium, caspase, catalase, cathepsin, legumain, NBR1, peroxisomes, pexophagy, ROS

Summary statement: The molecular mechanisms governing pexophagy have been elusive. The data presented in this study show that pexophagy takes place in response to Cd toxicity to regulate peroxisomal populations and quality and is regulated by H2O2, and peroxisomal oxidation. NBR1 may be an autophagic receptor for peroxisome and cathepsin B, legumain and caspase 6 could be involved in the regulation of pexophagy.

Abbreviations: ATG, autophagy gene; CAT, catalase; CFP, cyan fluorescent protein; DNPH, Dinitrophenylhydrazine; GFP, green fluorescent protein; NBR1, Neighbor of Brca1 gene 1; PEX, peroxine; ROS, reactive oxygen species

Introduction

Peroxisomes, which are organelles surrounded by a single membrane, contain catalase and hydrogen peroxide (H_2O_2)-producing flavin oxidases and are present in almost all eukaryotic cells. They are involved in metabolic pathways such as fatty acid β-oxidation, the glyoxylate cycle, photorespiration, ureide metabolism and biosynthesis of plant hormones including jasmonic acid, salicylic acid and auxin; they are also a highly important source of reactive oxygen (ROS) and nitrogen species (RNS) (Sandalio, Rodríguez-Serrano, Romero-Puertas & del Río, 2013). Peroxisomal ROS production is mainly associated with photorespiration, fatty acid β-oxidation and ureide metabolism (Sandalio & Romero-Puertas, 2015). Although ROS accumulation induces oxidative damage, these organelles contain a battery of antioxidants, including superoxide dismutase, which detoxifies the O_2^- radical catalase (CAT), and ascorbate-glutathione cycle enzymes, which remove H_2O_2 (Sandalio & Romero-Puertas, 2015). Peroxisomes therefore have the capacity to rapidly produce and scavenge H_2O_2 and O_2^-, which facilitates the regulation of dynamic changes in ROS and cellular redox status (Sandalio & Romero-Puertas, 2015).

Plant peroxisomes are highly dynamic organelles that adapt to environmental changes by altering their populations, although the molecular basis of plant peroxisome proliferation is not fully understood. The proliferation of peroxisomes involves a three-step process: peroxisome elongation, constriction and fission (Hu, 2010; Hu et al., 2012). Peroxisome proliferation in plants can be triggered by H_2O_2, Cd, Clofibrate, ozone, UV, salinity and light (Hu, 2010; Rodríguez-Serrano, Romero-Puertas, Sanz-Fernández, Hu & Sandalio, 2016; Sandalio et al., 2013). As an excessive amount of peroxisomes can produce severe disturbances in redox homeostasis (Nila et al., 2006; Sandalio & Romero-Puertas, 2015), the cell requires a mechanism to control the peroxisome population.

Autophagy is a conserved process which degrades and recycles unwanted cytoplasmic components such as biomolecules and organelles. It was first described in yeast and later in all eukaryotic organisms including plants (Li & Vierstra, 2012; Ohsumi, 2014). Although studies of autophagy in plants are less advanced than those in animals, its essential components and basic developmental machinery have been conserved (Avin-Wittenberg et al., 2018; Li & Vierstra, 2012; Liu & Bassham, 2012). There are three major autophagy pathways: macroautophagy, microautophagy and selective autophagy (Michaeli & Galili, 2014). In macroautophagy, the most studied type of autophagy, unwanted material is first engulfed by a double membrane structure called the phagophore, which eventually forms

double membrane vesicles, or autophagosomes, to transfer these materials to vacuoles where proteins and organelles are degraded (Avin-Wittenberg et al., 2018; Michaeli & Galili, 2014). In plants, macroautophagy plays an important role during crucial plant processes such as development, senescence, innate immunity, programmed cell death as well as biotic and abiotic stress responses (Avin-Wittenberg et al., 2018; Michali & Galili, 2014). In microautophagy, the tonoplast forms an invagination which directly engulfs the cargo to form an autophagic body which is degraded inside the vacuole (Li, Li & Bao, 2012; Michaeli et al., 2016; Van Doorn & Papini, 2013). Selective autophagy involves specific degradation and recycling processes for the following organelles: peroxisomes by pexophagy, mitochondria by mitophagy, the endoplasmic reticulum by reticulophagy and chloroplasts by chlorophagy (Kim et al., 2013; Li, Chung & Vierstra, 2014; Liu et al., 2012; Xie, Michaeli, Peled-Zehavi & Galili, 2015).

Autophagy (ATG) genes are required for the precisely regulated process of autophagy. In plants, these genes have been characterized in *Arabidopsis thaliana* (Doelling, Walker, Friedman, Thompson & Vierstra, 2002). ATG8, whose isoforms play an important role in autophagosome formation and functioning in all plant species studied, is a ubiquitin-like protein which is crucial at the early stages of autophagy (Michaeli et al., 2016). ATG8 proteins are initially localized on both sides of the phagophore, whose structure is initiated by the concurrence of ATG1 and ATG13 (Avin-Wittenberg et al., 2018; Li & Vierstra, 2012). The insertion of ATG8 into the phagophore membrane is mediated by different ligase-like proteins: ATG7, ATG3 and the ATG12-ATG5-ATG16 complex (Avin-Wittenberg et al., 2018; Li & Vierstra, 2012). The biogenesis of autophagosomes requires phosphatidylethanolamine (PE) conjugation to ATG8 proteins and previous post-translational processing of ATG8 by the cysteine protease ATG4 at the conserved C-terminal glycine (Gly) residue (Woo, Park & Dinesh-Kumar, 2014; Yoshimoto et al., 2004). Lipidated ATG8 interacts with cargo receptors to collect unwanted material which is then delivered to the vacuole for degradation (Avin-Wittenberg et al., 2018; Woo et al., 2014; Yoshimoto et al., 2004). The ATG4 protease is also necessary for the reverse de-conjugation step to remove ATG8-PE from the outer autophagosome membrane for ATG8 recycling and autophagosome completion (Woo et al., 2014). Plants contain multigene ATG8 and ATG4 families, which suggests that different functions depend on different conditions and tissues where autophagy is required or functional redundancy occurs (Kellner, De la Concepcion, Maqbool, Kamoun & Dagdas, 2017; Woo et al., 2014). Arabidopsis plants contain nine ATG8 isoforms

(ATG8a-ATG8i) and two ATG4s (ATG4a-ATG4b) (Kellner et al., 2017; Woo et al., 2014). Peroxisomes in different organisms can be degraded by a selective autophagic process called pexophagy, with both micro- and macro-autophagy processes also reported in plant tissues (Shibata et al., 2013; Till, Lakhani, Burnett & Subramani, 2012; Young & Bartel, 2016). Selective autophagic degradation of peroxisomes has recently been demonstrated by pharmacological and genetic experiments (Kim et al., 2013). Peroxisomes are selectively degraded by pexophagy during the functional transition of glyoxysomes to leaf peroxisomes (Kim et al., 2013). Oxidized peroxisomes have also been shown to be removed by pexophagy (Shibata et al., 2013; Yoshimoto et al., 2014). Shibata et al. (2013) have shown that peroxisomes appear to be aggregated and separated from chloroplasts and mitochondria in the leaves of Arabidopsis knockout *atg2*, *atg7* and *atg18a* mutants. These aggregated peroxisomes showed inactive catalase accumulations, suggesting that the oxidation of peroxisomal proteins can target peroxisomes for further degradation by pexophagy (Shibata et al., 2013). This finding is corroborated by the co-localization of ATG8 with aggregated peroxisomes (Yoshimoto et al., 2014). In a forward genetic screen for Arabidopsis mutants with altered peroxisomal positioning, evidence suggests that pexophagy is crucial for quality control mechanisms in Arabidopsis (Kim et al. 2013; Shibata et al., 2013; Yoshimoto et al., 2014). Evidence of peroxisomal degradation by bulk autophagy during carbohydrate starvation has been reported in tobacco BY-2 suspension culture cells (Voitsekhovskaja, Schiermeyer & Reumann, 2014). Interestingly, the subcellular localization of these peroxisomes changes positioning around the nucleus. The number of peroxisomes also decreases due to pexophagy during carbohydrate starvation up to the fourth day of starvation (Voitsekhovskaja et al., 2014).

Selective degradation of peroxisomes involves ATG8 and adaptor proteins which interact with both ATG8 and cargos. In plants, NBR1 (Neighbor of BRCA1 gene 1) and ATI1 (ATG8-interacting protein1) proteins interact with ATG8 and may play an important role as adaptors, thereby facilitating delivery of captured autophagy cargos to autophagosomes for degradation (Masclaux-Daubresse, Chen & Havé, 2017). However, the autophagic adaptor protein linking ATG8 to damaged or obsolete peroxisomes has not yet been identified. In mammalian cells, it has been suggested that polyubiquitination of some peroxisomal membrane proteins mobilizes p62 and NBR1 which act as autophagic adaptors to bind ATG8 (Oku & Sakai, 2010). In Arabidopsis plants, NBR1, a p62/NBR1 ortholog, targets ubiquitin-tagged proteins (Zhou et al., 2013). However, the role played by NBR1 as a plant pexophagy

receptor remains unclear; *nbr1* mutants, though not subject to early senescence, are highly sensitive to oxidative stress (Zhou et al., 2013), while no ubiquitinated proteins have been detected in peroxisomes (Yoshimoto et al., 2014).

The toxic heavy metal cadmium (Cd), which is present in the environment mainly due to anthropogenic activities such as metalworking industries, cement factories, smelting plants, refineries and phosphate fertilizer production, is then transferred to the food chain (Clemens et al., 2006). Cadmium inhibits plant growth as a consequence of alterations in the photosynthesis rate, macro- and micro-nutrient uptake and distribution and disturbances in antioxidant defenses (Rodríguez-Serrano et al, 2009; Romero-Puertas et al., 2018). In a previous study, we demonstrated that Cd induces peroxisome proliferation after three hours of treatment (Rodríguez-Serrano et al., 2016). The aim of this study is to determine whether this transient increase in peroxisomal populations under Cd treatment conditions is regulated by pexophagy and to identify the mechanisms involved in this process. We thus analyzed time course-dependent changes in the expression and protein accumulation of ATG8s, as well as the accumulation of PEX14 used as a peroxisomal marker. Through protein immunolocalization, we also evaluated the role of NBR1 as an autophagy receptor for peroxisomes. To identify the signal involved in triggering autophagy/pexophagy under these conditions, we studied total protein carbonylation and the redox state of peroxisomes by imaging H_2O_2 in these organelles. The contribution of ROS from NADPH oxidase (RBOH) and glycolate oxidase (GOX) in promoting pexophagy has also been analyzed in Arabidopsis *rbohC* and *gox2* mutants. The possible role played by the different proteases was also analyzed. Our results suggest that pexophagy plays a significant role in rapid cell responses to cadmium to regulate peroxisomal populations, a process which could be regulated by NBR1 and triggered by oxidation of peroxisomal proteins such as catalase.

MATERIALS AND METHODS

Plant Material, Growth Conditions and Treatments

Arabidopsis thaliana ecotype Columbia-0 (Col-0) constitutes the genetic background for all wild-type plants used in this study, except for *atg7* mutants, which were obtained with a Wassilewskija (Ws) background. Wild type plants expressing GFP-ATG8a, as well as Arabidopsis T-DNA disruption mutants affecting *atg5* and *atg7* were kindly supplied by Dr.

Vierstra (Washington University, St Louis, USA) and Henri Batoko (University of Louvain, Belgium), respectively. We selected *atg5* and *atg7,* as they are among the best characterized autophagy-deficient mutants in Arabidopsis and are encoded by a unique gene. Arabidopsis lines *rbohC* and *gox2* were obtained from the SALK and NASC collections. Arabidopsis lines, simultaneously expressing peroxisomal markers CFP-SKL and GFP-ATG8a, were obtained by cross-pollinating *px-ck* Arabidopsis lines (Nelson, Cai & Nebenführ, 2007) with GFP-ATG8a lines (Thompson, Doelling, Suttangkakul & Vierstra, 2005) and by selecting double homozygous lines (Fig. S1). The presence of CFP in peroxisomes was checked in leaves with the aid of a fluorescence microscope. Genomic DNA from leaf discs was then extracted, and PCR screening was carried out using primers specific to the CaMV 35S promoter and ATG8a (Table S1). Arabidopsis seeds were surface-sterilized and stratified for 48 h at 4°C and then sown on Murashige & Skoog (MS) 0.5x solid medium (Murashige & Skoog, 1962) containing 3% sucrose (w/v) and 0.8%, phytoagar (w/v). The plants were then grown at 22°C in 16 h light and 8 h darkness for 10 d, transferred to Petri dishes with 0.5x liquid MS medium containing sucrose and then grown for 24 h. They were treated with 100 µM $CdCl_2$ at different times (0.5 h, 3 h, 6 h, 9 h, 15 h and 24 h), with untreated plants (0 h) used as control.

qRT-PCR analysis of gene expression

Total RNA was isolated from whole 10 day-old seedlings using the acid guanidine thiocyanate-phenol-chloroform method, as described by Chomczynski and Sacchi (1987), and the RNeasy Plant Mini Kit (Quiagen) for gene expression analyses. RNA was reverse transcribed using an oligo (dT) primer and the Invitrogen SuperScript First-Strand Synthesis System for RT-PCR (Life Technologies) according to the manufacturer's instructions. Quantitative real-time PCR was performed on an iCycler iQ5 (Bio-Rad, Hercules, CA, USA). Each 20 µl reaction contained either 1µl o cDNA or a dilution, 200 nM of each primer and iQ SyBrGreen Supermix (BioRad). Control PCR reactions of the RNA samples not treated with reverse transcriptase were also carried out to confirm the absence of contaminating genomic DNA. The samples were initially denatured by heating at 95° C for 3 min followed by 45-cycle amplification and a quantification program (95° C for 30 s, 55° C for 30 s, 60° C for 1 min and 72° C for 45 s). A melting curve was conducted to ensure amplification of a single product. Amplification efficiency was calculated using the formula E = [10 (1/*a*) -1] × 100, where *a* is the slope of the standard curve. The relative expression of each gene was normalized to that of *TUB2* or *UBQ10*, and the results were analyzed using the method

described by Pfaffl (2001). The primers used are described in Table S1. Any increase of over 1.5 was considered to constitute up-regulation.

Western blot analysis

Whole 10-day-old seedlings were homogenized in liquid nitrogen in Eppendorf tubes with a micro pestle using different protein extraction buffers and centrifuge conditions depending on the protein of interest.

For ATG8a identification, whole plants (100-200 mg) were homogenized in 100 mM Tris-HCl, pH 7.5, 400 mM sucrose, 1 mM EDTA, 10 mg mL-1 sodium deoxycholate, 0.1 mM phenylmethylsulfonyl fluoride, 10 mg mL-1 pepstatin A and 4 % [v/v] protease inhibitor cocktail [Roche] centrifuged at 500 g for 10 min to obtain the supernatant fraction as described previously (Álvarez et al., 2012). For immunoblot analysis, 40-60 μg of leaf protein extracts was electrophoresed on 15 % acrylamide gels. For PEX14, the same buffer, but without pepstatin A, was used in a 1:2 (w/v) ratio. The extract was centrifuged at 15890 g for 30 min at 4 °C, and 40-60 μg of proteins from the extracts were loaded for SDS–PAGE (10% polyacrylamide).

The electrophoresed proteins were then transferred to a polyvinylidene fluoride membrane (Millipore Co., Bedford, MA, USA) in a Bio-Rad Semi-Dry Transfer Cell (Bio-Rad, Hercules, CA, USA). The membranes were incubated for 1 h in blocking buffer containing 3 % milk powder (w/v) prepared in TBS containing 0.1 % Tween 20 (v/v). Antibodies were diluted in blocking buffer; anti-At-ATG8 (Abcam, Cambridge, UK) was diluted 1:2000 and anti-PEX14 (Agrisera) 1:10000. Membranes were washed with TBS and incubated with goat anti-rabbit IgG conjugated with HRP (Agrisera; 1:20000-1:50000 in blocking buffer). After washing with TBS, bands were visualized by the ECL Western blot detection system (GE). The immunodetected protein bands were quantified relative to the Ponceau or SYPRO Ruby-stained membrane using ImageJ software.

Protein concentration in the extracts was measured by means of the Bradford protein assay (Bio-Rad) using bovine serum albumin (BSA) as standard.

Immunochemical detection of carbonylated proteins

According to the method described by Romero-Puertas, Palma, Gómez, Del Río and Sandalio (2002), carbonyls were detected by protein derivatization with dinitrophenylhydrazine (DNPH, Sigma; Suppl. Material and Methods)

Confocal microscopic analyses

ATG8 and peroxisome detection

To avoid GFP fluorescence loss during confocal microscopy analysis, the seedlings were incubated in liquid MS medium (with 3% sucrose) containing 0.5 μM concanamycin A (Santa Cruz Biotechnology) for 16 h at room temperature in the dark before treatment with cadmium. Arabidopsis plants expressing GFP-ATG8a (Exc/Em: 488/508 nm) were examined using a Nikon C1confocal laser scanning microscope to monitor autophagy after 30 min, 3 h, 6 h and 9 h $CdCl_2$ (100 μM) treatments. Images of cadmium-treated plants, which were obtained as 20-25 z-steps in 0.4 μm intervals by confocal microscopy, were combined using maximum intensity projection. An optimal pinhole of 1 Airy disk size was used and a 488 nm excitation laser and 590/50 nm detector were used. Gain was adjusted to avoid saturation.

To analyze pexophagy, seedlings simultaneously expressing CFP-SKL (Exc/Em: 434/476 nm) as peroxisome marker and GFP-ATG8a (Exc/Em: 488/508 nm) as autophagy marker were used. A Leica sp5 spectral confocal microscope was used for this purpose. For CFP, a 405 nm diode was used for detection, with excitation set to 467 and emission to 490 nm. For GFP, a 496 nm diode was used with excitation at 505 and emission at 529 nm. An optimal pinhole of 1 Airy disk size was used.

H_2O_2 accumulation in peroxisomes: image acquisition and processing

To image H_2O_2 accumulation in peroxisomes, Arabidopsis lines expressing the H_2O_2 biosensor HyPer in these organelles were used (seeds supplied by Dr. A. Costa; Costa et al., 2010). All analyses were carried out on leaves from untreated plants (control) and from plants treated with 100 μM $CdCl_2$ for 4 h. For image acquisition, a Nikon A1Si confocal microscope equipped with a 40x lens was used. Intensity ratio image data were obtained with the aid of one-way sequential line scans of two excitation lines. To measure the effect of Cd treatments on HyPer oxidation (indicated by an increased 488/455 nm excitation ratio), the 488/405-nm

laser power ratio was kept constant at 1:3 and emission was collected with a detector at 540/530 nm, with a photomultiplier tube gain of 90–120 AU. No offset was used, and pinhole size was set at between 1.2 and 2 times the Airy disk size of the objective used depending on signal strength. Chloroplast autofluorescence was imaged with excitation at 640 nm and emission at 670–720 nm.

The images were analyzed according to the method described by Mishina et al. (2013). Briefly, images were smoothed using a Gaussian filter, and pixels containing the biosensor signal were separated from the background according to Otsu's method (Otsu, 1979). A ratio image, which was created by dividing the 488 nm image by the 405 nm image pixel by pixel, was displayed using false colors.

Plant tissue processing for transmission electron microscopy and immunolabeling

Leaves were fixed in 4% formaldehyde and 0.25% glutaraldehyde with 50 mM cacodylate buffer (pH 7.2) at 4°C for 3 h. For proper fixative penetration, vacuum was applied 3 times for 10 min, fresh fixative was added, and samples were continuously shaken at 4°C overnight. After fixation, all samples were washed in 50 mM cacodylate buffer, pre-embedded in 0.8% low melting agarose, dehydrated in ethanol series and embedded in Unicryl. After resin polymerization, ultrathin sections were obtained. Catalase was localized using a specific anti-catalase antibody (Agrisera, Sweden), diluted 1/500 in PBS pH 7.4 containing 0.1% BSA and 0.005% Tween 20 (1 h incubation). NBR1 and ATG8a were immuno-labelled using antibodies against NBR1 (1/1000 dilution; Agrisera, Sweden) and anti-At-ATG8a (1/1000 dilution; Abcam, Cambridge, UK), respectively (1 h incubation); goat anti-rabbit IgG conjugated to 15 nm gold particles was used as a secondary antibody (1/50 dilution) (Sandalio, López-Huertas, Bueno & del Río, 1997). Double immunogold labelling of catalase and ATG8, as well as ATG8 and NBR1, was carried out using goat-anti-rabbit IgG conjugated to 5 and 15 nm gold particles to identify individual proteins. Sections were post-stained for 20 min in 2% (w/v) uranyl acetate and were then examined with the aid of a JEOL JEM-1011 transmission electron microscope.

Peroxisome cytochemistry and microscopy analysis

The method used was essentially that reported by Nila et al. (2006). Pieces of leaves (1 mm^2) were vacuum-infiltrated for 10 min three times with 0.5% (v/v) glutaraldehyde in 50 mM phosphate buffer, pH 6.8, and incubated for 3 h at room temperature. Leaf samples were then

washed three times with buffer and incubated at 37 °C with a solution containing 3,3'-diaminobenzidine (DAB, 2 mg/mL) in 50 mm Tris-HCl buffer, pH 9, in the dark for 1.5 h. The tissue was then incubated for 3 h in the DAB solution supplemented with 0.02% (v/v) H_2O_2. After staining, leaf samples were washed with 50 mM phosphate buffer, pH 6.8, and stained with 1% (w/v) OsO_4. Leaf samples were then dehydrated in a graded ethanol series (30–100%; v/v), embedded in Embed 812 resin series (25–100%; w/v) (Electron Microscopy Sciences, Hatfield, PA, USA) and cut into thin (0.5–0.7 mm) or ultra-thin (50–70 nm) sections for further optical and electron microscopy analysis. The sections were not stained for optical microscopy analysis, but were post-stained with uranyl acetate for electron microscopy analyses. The plants used were Arabidopsis Col 0 (WT), *atg5*, WS and *atg7*.

Protease activity of Arabidopsis protein extracts after treatment with CdCl₂

Protease activity was quantified in untreated (C) Arabidopsis whole plants and after treatment with CdCl₂ for 30 min, 3 h, 6 h, 9 h 15 h and 24 h. Plants were collected and frozen (-20ºC) until needed. Total protein extracts from the Arabidopsis seedlings were ground and resuspended in 0.15 M NaCl sodium phosphate (pH 6.0) and 2 mM EDTA using sand and centrifuged at 15890 g for 5 min; the supernatants were pooled to obtain soluble protein extracts for enzymatic activity assays. For assays, 20 µg of plant protein extract was used, and the corresponding substrate was added to a final concentration of 0.25 mM for cathepsins and caspases and 0.8 mM for legumains. Cathepsin B-,L-like and legumain cysteine proteases and caspase 1 and 6 activities were assayed using Z-RR-AMC (Bachem), ZFR-AMC (Bachem), ZAAN-AMC (Bachem), Ac-YVAD-AMC (Enzo) and Ac-VEID-AMC (Enzo) substrates, respectively. The reactions were incubated in a buffer containing 100 mM sodium phosphate (pH 6.0), 10mM L-cysteine, 10 mM EDTA and 0.01% (v/v) Brij 35 for cysteine proteases (cathepsin B-, L-like and legumain) and 50 mM HEPES (pH 7.0), 0.5 mM DTT, 0.1% CHAPS, 50 uM PMSF and 5 uM pepstatin A for caspase 1 and 6. For legumain assays, the buffer contained 1mM DTT. Fluorescence was measured using 365 nm excitation and 465 nm emission filters (Tecan GeniusPro). The system was calibrated with known amounts of AMC hydrolysis product in a standard reaction mixture. Specific enzymatic activity was calculated as moles of substrate hydrolyzed/min/mg protein. All assays were carried out five times, and blanks were used to account for spontaneous breakdown of substrates.

Statistical analysis

The mean values in the experiments described above were obtained from at least three replicates from three independent experiments. Statistical analyses were performed using an ANOVA test with the aid of Statistic 8 software. Mean values for the different treatments were compared using Tukey's multiple comparison test ($p < 0.05$) and Dunn's Method (*$p < 0.001$) and the T Student test (*$p < 0.05$; **$p < 0.01$; *** $p < 0.001$).

RESULTS

Cadmium induces oxidative stress and selective autophagy

Although cadmium is a non-essential element it can be easily taken up by plants through essential nutrients transporters such as Fe, Zn, and calcium (Ca; Clemens, 2006). The best-studied transporters associated with Cd entrance, include IRT1, a member of the large ZIP (for Zinc-regulated transporter 1/IRT1-like Protein) family, which is the main entry vehicle for Fe^{2+} in Arabidopsis roots (Grotz and Guerinot, 2006) and the Nramp (natural resistance-associated macrophageprotein) family (Clemens and Ma, 2016; Loix et al., 2017). In particular, AtNRAMP3 and AtNRAMP4 function in the release of metals, including Fe and Cd, from the vacuole having a critical role under Cd and oxidative stresses (Nevo and Nelson, 2006; Molins et al., 2013). To understand the temporal kinetics of events linked to Cd-stress responses we have analysed the expression level of *IRT1* and *NRAMP3* which showed differential responses to the metal, with up-regulation of *IRT1* only occurring after 3 h of treatment, while no significant changes were observed in *NRAMP3* expression levels (Figure 1A). To determine the effect of Cd on ROS metabolism, we analysed oxidative markers after 3 and 15 h of cadmium treatment (100 μM), which showed a significant increase in *GST* expression levels after 3 h of Cd treatment. No changes were observed after 15 h, with neither of these time periods showing any change in *CAT2* expression (Fig 1 B).

In a previous study (Rodríguez-Serrano et al., 2016), we observed that Cd induces peroxisome proliferation in Arabidopsis leaves after 3 h of treatment, although the number of peroxisomes was similar to that in control plants after 24 h. To determine whether Cd induces autophagic processes to regulate peroxisomal populations, we first carried out a time course analysis of autophagic markers in whole Arabidopsis seedlings between 30 min and 24 h of Cd treatment. We analysed the transcript levels of the autophagy-related gene 8 (ATG8)

family composed of 9 members (*ATG8a* to *8i)* (Sláviková et al., 2005). After 3 h of exposure to Cd, the transcript levels of *ATG8h*, followed by *ATG8c*, *a* and *i*, were slightly up-regulated and returned to normal after further exposure to Cd (15 h) (Fig. 2). To demonstrate the induction of autophagy, ATG8a protein levels were analysed by immunoblot analysis using an ATG8a-specific antibody, and the time course analyses were also extended from 6h to 9h of treatment. Like gene expression, ATG8 protein levels increased after 3 h of Cd treatment, with the highest levels observed after 6 h of exposure (Fig. 3A). However, analysis of the expression levels of the other autophagy marker, *ATG7*, showed no significant changes between 0.5 h and 9 h of Cd treatment (Figure S2).

To determine whether autophagy selectively affects peroxisomes, we analysed changes in the accumulation of peroxine 14 (PEX14), a protein associated with the peroxisomal membrane. Time course analysis showed increased PEX14 protein accumulation after 3 hours of Cd treatment (Fig. 3B), which is in line with the increase in the peroxisomal population observed by confocal analysis in a previous study (Rodríguez-Serrano et al., 2016). PEX14 content subsequently decreased at between 6 and 9 h of treatment and then increased at between 15 and 24 h of exposure (Fig. 3B), a pattern opposite to that observed for ATG8 accumulation (Fig. 3A), which could explain the reduction in peroxisomes in leaves after longer Cd exposure. The reduction in PEX14 at between 6 and 9 h of treatment was considerably attenuated in Arabidopsis lines *gox2* (Fig. 3C) and *rbohC* (Fig. 3D), which showed disturbances in H_2O_2 production in response to Cd associated with peroxisomes (unpublished results) and the plasma membrane (Rodríguez-Serrano et al., 2016; Gupta et al., 2017), respectively.

To clearly demonstrate pexophagy, we obtained Arabidopsis lines constitutively expressing both ATG8a-GFP and CFP-labelled peroxisomes (GFP-SKL). Using confocal microscopy, we imaged the formation of phagophores and peroxisomes in leaves from plants treated with concanamicine A for 16 h to avoid GFP degradation in the vacuoles (Thompson et al., 2005) before treatment with 100 μM Cd. As shown in Fig. 4 B, after 6 h of Cd treatment, a 30% of peroxisomes (number of pictures=29) showed colocalization with phagophores, while no significant colocalization (less than 4%) was detected in control plants (Fig 4A), thus demonstrating that Cd induces pexophagic degradation of specific peroxisomes.

ATG8a was also immunogold-localized in cross sections of leaves from plants treated with Cd for 6 h and analysed using electron microscopy (Fig. 5 A, B and D). To identify

peroxisomes, we used catalase antibodies (Fig. 5 A). ATG8a colocalized with catalase present in the peroxisomal core (Fig. 5 A) and was also localized in peroxisomes close to the electron-dense core associated with electron-lucent spaces surrounding the peroxisome (Fig. 5B) identified as the autophagosome (Yoshimoto et al., 2014). With regard to the identity of proteins which recognize peroxisomes, immuno-localized NBR1 and gold particles associated with electron-lucent spaces surrounding the peroxisome were located close to the peroxisomal membrane (Fig. 5 C). Given that NBR1 has been shown to interact with ATG8, we also immuno-localized both NBR1 and ATG8a in Arabidopsis leaves and observed co-localization of both proteins mainly close to the electron-dense core inside the peroxisome (Fig. 5 D, D'). These results suggest that NBR1 might interacts with ATG8 and an, as yet, unidentified peroxisomal protein, which would enable the peroxisomes to be degraded during stress caused by cadmium treatment to be recognized. Given the localization of ATG8 close to the electron-dense core and co-localization with catalase in these cores (Fig. 5 A), oxidized catalase could be a peroxisomal target of pexophagy. However, physical interactions between catalase and NBR1 or catalase and ATG8a are unlikely, and an intermediary peroxisomal membrane protein, as yet undetermined, is probably involved in recognizing the peroxisomes to be degraded.

To distinguish between macrophagy and microphagy, peroxisomal accumulation in Arabidopsis mutants deficient in ATG5 was analysed. Thus, peroxisomes were stained with DAB and imaged by light and electron microscopy after 15 h of Cd treatment. As shown in Figure 6 (A, B and I), after 15 h of Cd treatment no significant changes were observed in the total number of peroxisomes or in the pattern of peroxisome accumulation in WT Col 0 plants (Fig. S3). However, under control conditions, accumulation of peroxisomes was observed in *atg5* Arabidopsis mutants as compared to WT plants (Fig 6 E-F; Fig S3), while the number of total peroxisomes increased considerably in *atg5* mutants after 15 h of Cd treatment parallel to changes in the pattern of peroxisomal aggregation (Fig. 6 G-H, J; Fig S3). The number of peroxisomes in *atg7* mutants after 15 h of Cd treatment (Fig. S4 A), as well as peroxisome aggregation (Fig S4B), increased significantly, while a slight reduction in peroxisomes was observed in WS plants under the same conditions (Fig S 4A). These results demonstrate that selective autophagy is induced by Cd in order to regulate peroxisomal populations. Peroxisomes, which were more pleomorphic in Cd-treated *atg5* lines (Fig. 6 F), were of different sizes, although mean area was slightly greater than in untreated WT. Another characteristic of peroxisomes in *atg5* under Cd treatment conditions was the

presence of polar electron-dense structures and small spots surrounding the surface of the organelle (Fig. 6 H), possibly due to excess H_2O_2, which also reacts with DAB.

Oxidized proteins induce autophagy and pexophagy

The signal involved in autophagy induction in plants has not been precisely identified. Given that ROS and oxidative protein modifications have been shown to induce autophagy, we analysed oxidized proteins at different Cd treatment times using DNPH and specific anti-DNP antibodies. Cd promotes protein oxidation after 3 h of treatment, with maximum oxidation observed after 9 h of exposure (Fig. 7A and B). To determine whether peroxisomal oxidation targets these organelles for pexophagic degradation, we analyzed H_2O_2 accumulation in peroxisomes by using Arabidopsis lines constitutively expressing the biosensor HyPer in these organelles. This biosensor, which allows monitoring changes in H_2O_2 levels specifically in peroxisomes, is a marker of peroxisomal redox state. Under control conditions, although fluorescence associated with HyPer was mainly observed in peroxisomes, a weak signal was also detected in the cytosol (Fig. 8A). After 4 h of Cd treatment, a significant increase in the number of peroxisomes was observed (Fig. 8 B), which is in line with previously reported results (Rodríguez-Serrano et al., 2016) and with the increase in PEX14 accumulation observed after 3 h of treatment in this study. A significant increase in H_2O_2-accumulating peroxisomes and H_2O_2 content was observed as compared to untreated plants (Fig. 8 C-E). The images also show H_2O_2 accumulation in specific micro-domains of the peroxisomal matrix. The cytosol also showed an increase, though non-significant, in H_2O_2 in response to Cd (Fig. 8E). These results demonstrate that Cd induces peroxisomal oxidation and suggest that a specific oxidized peroxisomal protein could be targeted by NBR1 and ATG8 in order to promote pexophagy.

Proteolysis is involved in cadmium-induced autophagy

In addition to autophagy, several proteases could be involved in regulating protein content and quality under stress conditions. To determine the role of these proteases in response to Cd, we analyzed the major proteolytic activity profiles using specific substrates. Caspase 6-like protease activity increased between 3 and 6 h of Cd treatment, while caspase 1-like protease activity remained virtually unchanged (Fig. 9). Although cathepsin L was unaffected, a reduction in cathepsin B activity was observed during Cd treatment (Fig. 9). An increase in legumain activity was observed after 9 and 15h of Cd treatment (Fig 9). These

results demonstrate that proteolysis could play an important role during the Cd treatment periods analyzed, with changes observed in the pattern of different proteases.

Discussion

Cadmium causes severe plant growth inhibition and even cell death in various plant species (Iakimova, Woltering, Kapchina-Toteva, Harren & Cristescu, 2008). It also produces alterations in the membrane, photosynthesis rates, plant/water balance and in macro- and micro-nutrient distribution (Gupta et al., 2017; Sandalio et al., 2013; Zhang & Chen, 2011). Biochemical and molecular analyses carried out under Cd stress conditions suggest that oxidative stress is one of the primary effects of exposure to Cd, which promotes lipid peroxidation and protein oxidation (Djebali et al., 2008; Paradiso et al., 2008; Pérez-Chaca et al., 2014; Sandalio, Dalurzo, Gómez, Romero-Puertas & del Río, 2001). In addition to their harmful effect on molecules, ROS, particularly H_2O_2, also regulate cell responses to Cd (Romero-Puertas, Ortega-Galisteo, Rodríguez-Serrano & Sandalio, 2012). However, although considerable information exists on Cd toxicity in plants exposed to long periods of Cd treatment, less is known about the effect of short periods of treatment. In this study, we observed that Cd promotes rapid *IRT1* up-regulation which could increase Cd up-take during the first hours of treatment. Parallel to *IRT1*, *GST* upregulation was also observed, thus demonstrating Cd-dependent of oxidative stress conditions.

Information on the involvement of selective and non-selective autophagy in Cd toxicity is particularly scarce. On the other hand, the induction of autophagy in plants has been shown to occur during nutrient starvation and under abiotic stress conditions including heat, salinity, drought and oxidative stress (Avin-Wittenberg et al., 2018; Cheng et al., 2016; Liu, Xiong & Bassham, 2009; Pérez-Pérez, Lemaire & Crespo, 2012). In this study, we analyzed the effect of Cd on the selective autophagy of peroxisomes (pexophagy) in response to short periods of treatment. Arabidopsis plants contain nine different *ATG8* isoforms (a-i; Kellner et al., 2017). Time course analyses of the expression of all *ATG8* genes present in Arabidopsis plants, which are regarded as the principal markers of autophagy, have shown transient up-regulation of several *ATG8s*, mainly *ATG8h*, followed by *ATG8c,* a and *i,* after 3 h of Cd treatment, while longer treatment periods (15 and 24 h) left their expression unchanged. Differential regulation of *ATG8* expression under nitrogen starvation conditions has been reported in Arabidopsis plants, with *ATG8i* being the most prominent, followed by *ATG8d, ATG8c, ATG8a* and *ATG8e* (Yoshimoto et al., 2004). We also confirmed that ATG8 protein

accumulation increased between 3 to 9 h of Cd treatment. However, the expression of *ATG7* did not change significantly in the first 9 h of treatment. Differences in *ATG7* and *ATG8a* expression have been also observed in Arabidopsis plants exposed to high temperatures (Zou et al., 2013). However, we cannot rule out the possibility that the ATG7 protein is regulated by post-translational modifications (PTMs), as has been reported for ATG4 which is regulated by redox reactions (Pérez-Pérez et al., 2014). However, no information is available on specific PTMs of ATG7, although ATG7 and ATG5 have been reported to be regulated by acetylation in mammalian cells (Bánréti, et al., 2013). Although *ATG8* diversification in plants is not fully understood, it has been suggested that individual *ATG8* family members in Arabidopsis plants function under specific developmental conditions or in response to specific stimuli to target specific cargos for degradation, as *ATG8* genes are differentially expressed in organs, tissues and cell types under different stress conditions (Kellner et al., 2017; Yoshimoto et al., 2004; Woo et al., 2014).

Using LysoTracker Green DND-26 as a marker of autophagosome-related structures, Cd has been reported to induce cell death through autophagy in Arabidopsis plants, although more specific autophagy markers have not been analysed (Zhang & Chen, 2011). Cadmium induces autophagy in mammalian cells, which produces ROS, although the molecular mechanism involved is unclear (Liu et al., 2016; Son et al., 2011). In a previous study, we demonstrated that peroxisomes can act as sensors of Cd-induced H_2O_2, which causes changes in the dynamics of these organelles (Rodríguez-Serrano et al., 2016). Thus, after 30 minutes of Cd treatment, the organelles produce dynamic extensions, called peroxules, which are involved in regulating H_2O_2 accumulation and ROS-dependent signalling transduction (Rodríguez-Serrano et al., 2016). The formation of these structures is transient and is followed by elongation and further peroxisome proliferation. However, after 24 h of treatment, peroxisome populations were similar to those observed in control plants, while their velocity of movement increased (Rodríguez-Serrano et al., 2009; Rodríguez-Serrano et al., 2016). These changes in peroxisomal dynamics have been reported to be related to the regulation of rapid cell responses to environmental cues (Rodríguez-Serrano et al., 2016). As excess peroxisomes can produce severe disturbances in redox homeostasis (Nila et al., 2006; Sandalio & Romero-Puertas, 2015), cells require a mechanism to maintain peroxisome populations under control. It has been suggested that autophagy plays an important role in controlling peroxisomal quality in plants through selective degradation of oxidized peroxisomes (Kim et al., 2013; Shibata et al., 2014). Using different Arabidopsis *atg* mutants,

peroxisomes have been observed to accumulate in hypocotyls and leaves, though not in roots, suggesting that a specific type of pexophagy is present in these tissues, probably due to the greater extent of oxidative damage detected in green tissues, where β-oxidation and photorespiration play a prominent role in ROS production (Shibata et al. 2013; Yoshimoto et al. 2014; Young & Bartel, 2016). To understand how cells regulate the abundance of peroxisomes under Cd toxicity conditions, we obtained Arabidopsis mutants expressing GFP-ATG8a and CFP-SKL; by imaging autophagosomes and peroxisomes simultaneously, we observed that Cd treatment promotes the formation of phagophores surrounding certain peroxisomes, which are thus subject to a specific type of pexophagic degradation. Using electron microscopy, we also observed electron-lucent spaces surrounding some peroxisomes, identified as phagophores in a previous study (Yoshimoto et al., 2014; Fig 5 B, C). Time course analysis of peroxisomal marker PEX14 showed a pattern opposite to that observed for the ATG8 protein, with PEX14 increasing after 3 h of Cd treatment and decreasing after 6-15 h of exposure. These results corroborate the time-dependent Cd-induced pexophagic degradation of peroxisomes. Significant levels of peroxisome accumulation and clustering in Cd-treated *atg5* and *atg7* Arabidopsis mutants as compared to untreated WT, *atg5* and *atg7* mutants clearly demonstrate that Cd induces peroxisome proliferation and that cells are capable of regulating excess peroxisomes through selective autophagy. Neither the pexophagy-specific components in plants nor the peroxisomal targets involved in pexophagy induction, which is a major milestone in this field of research, have been clearly identified. In Arabidopsis *atg* mutants, Yoshimoto et al. (2014) observed an increase in peroxisomes and electron-dense regions inside organelles containing inactive insoluble catalase and immunolocalized ATG8 in electron-lucent structures identified as the seeds of isolation membranes close to the peroxisomal electron-dense core (Yoshimoto et al., 2014). For our part, we detected ATG8 immunogold signals associated with peroxisomes, mainly close to the electron-dense structures. Substantial evidence indicates that NBR1 acts as an ATG8-linked adaptor protein (Kalvari et al., 2014; Xie et al., 2016). In tobacco leaves infiltrated by *Agrobacterium tumefaciens,* ATG8 interacts with NBR1 through bimolecular fluorescence complementation (BiFC), while autophagy-deficient *nbr1* plants have been found to be more sensitive to oxidative stress (Zhou et al., 2013). A double NBR1 mutant (*nbr1-1*) unable to bind ATG8 *in vitro* or *in vivo* is compromised in terms of heat tolerance, indicating that interactions between ATG8a and NBR1 are necessary for autophagy to occur (Zhou et al., 2013). Our results corroborate the interaction of ATG8 and NBR1, which co-localize mainly in the area close to the electron-dense core of peroxisomes. Our findings suggest that

pexophagy involves ATG8a and NBR1. As putative mechanism, NBR1 could recognise ubiquitinated peroxisomal proteins as cargo, binds ATG8 through its conserved LIR motif (Waters et al., 2009, Svenning et al., 2011), thus selecting peroxisomes for degradation during Cd-induced stressful condition. It has been suggested that non-functional catalase, which accumulates in *atg2* mutants, is the target of peroxisomes to be degraded (Kim et al., 2013). Catalase aggregates are preferentially accumulated in Arabidopsis *nbr1* mutants which support possible NBR1/catalase interactions (Zou et al., 2013). However, one study of *atg2 cat2 cat3* triple mutants, with no detectable catalase, has reported the presence of peroxisome clusters (Shibata et al., 2013). On the other hand, our results indicate that catalase may be a target for pexophagy, although other proteins present in the peroxisomal electron-dense core or in the peroxisomal membrane close to these cores could be involved in targeting peroxisomes for autophagy. Recently, nine Arabidopsis PEX proteins containing short ATG8 interacting motifs (AIMs) have been identified, while bimolecular fluorescence complementation (BiFC) studies have confirmed that AtPEX6 and AtPEX10 interact with ATG8 (Xie et al., 2016). Direct interactions between ATG proteins and peroxisomal receptors without the participation of NBR1 cannot therefore be ruled out. In mammalian tissues, ROS-induced pexophagy is regulated by the ATM-dependent phosphorylation of peroxine PEX5 at Ser 141, which promotes PEX5 mono-ubiquitylation recognized by the autophagy adaptor protein p62 (Zhang et al., 2015). These putative PEX proteins, possibly involved in targeting pexophagy in plants, therefore require more in-depth study.

Although the signalling events that trigger plant pexophagy pathways have not yet been characterized, considerable evidence from different organisms points to oxidative changes as a key factor (Pérez-Pérez et al., 2012; Yoshimoto et al., 2014; Zhang et al., 2015). After analyzing carbonylated proteins during different treatment periods, we observed that the pattern of protein oxidation coincides with that for ATG8 and the peroxisomal marker; as previously reported in plants, humans and Chlamydomonas, this demonstrates that redox changes in cellular protein oxidation are involved in autophagy induction (Pérez-Pérez et al., 2012). In Arabidopsis leaves, exogenous applications of H_2O_2 induce oxidative damage to peroxisomes which are selectively degraded by autophagy (Shibata et al., 2013). In this study, using a specific H_2O_2 biosensor, we demonstrate that Cd induces a significant increase in H_2O_2 accumulation after 4 h of treatment. Judging by the results observed in *gox2* mutants, glycolate oxidase could be an important peroxisomal source of H_2O_2 involved in peroxisome proliferation and degradation in response to Cd. In pea leaf peroxisomes, Cd induces

glycolate oxidase activity as well as H_2O_2 accumulation (McCarthy et al., 2001). In mammalian cells, peroxisomal ROS induced by clofibrate treatment caused pexophagy (Zhang et al., 2015), although other sources, such as NADPH oxidases, could also be involved. In our study Arabidopsis *rbohC* mutants were found to slow down degradation of peroxisomes, while NADPH oxidases have been reported to be needed to regulate autophagy induced by starvation and salinity (Liu et al., 2009). Under control conditions, Yoshimoto et al. (2014) have reported that the redox status of some peroxisomes in Arabidopsis *atg5* mutants is disturbed, resulting in a more oxidized state than that of wild type mutants. In our study, electron-dense spots were found on the surface of peroxisomes in *atg5* mutants, which is compatible with H_2O_2 accumulation, which is in line with the findings of Yoshimoto et al. (2014), suggesting the presence of a non-active oxidized catalase in *atg5* mutants. Interestingly, using HyPer, we found that not all peroxisomes have similar H_2O_2 accumulation rates, and a H_2O_2 gradient was observed inside the peroxisomes (Fig. 8). In a previous study of Cd-treated pea plants, using $CeCl_3$ cytochemistry, a similar H_2O_2 gradient was observed in these organelles (Romero-Puertas et al., 2004). The presence of H_2O_2 gradients inside peroxisomes suggests a functional distribution of H_2O_2-producing peroxisomal proteins and antioxidants, although we were unable to determine the cause of this specific distribution.

Recent studies show that there is a link between autophagy and proteolytic systems in plants (Bárány et al., 2018; Bozhkov & Jansson, 2007; Hofius, Munch, Bressendorff, Mundy & Petersen, 2011; Minina et al., 2013). Cathepsin B and autophagy are involved in regulating hypersensitive cell death induced by pathogens (Hofius et al., 2011). PCD in Arabidopsis cathepsin B triple mutants has been shown to decrease sharply due to ultraviolet (UV), oxidative stress (H_2O_2, methyl viologen), endoplasmic reticulum stress and hypersensitive cell death (Ge et al., 2016). A correlation between cathepsin activity and autophagy has been reported after microspore embryogenesis was triggered in barley, although the connections between these two processes require further analysis (Bárány et al., 2018). Unlike plant responses to pathogens, our results show an opposite pattern for cathepsin B activity and ATG8 protein accumulation, suggesting that autophagy and cathepsin B degradation played an antagonistic role under our experimental conditions, although more in-depth studies will be needed to establish the molecular mechanisms involved. A recent proteomic study revealed an accumulation of cathepsin B3 in *atg5* mutants under both low and high nitrogen growth conditions as compared to control (Havé et al., 2018)

Legumains are a family of plant Asn-specific cysteine proteinases involved in Asn-specific propolypeptide processing and protein degradation in the vacuole. Their activity is controlled by the conformational state of their substrates, which undergo development- and environment-dependent changes (Müntz & Shutov, 2002). These proteases exhibit tertiary homology to caspases and are characterized by legumain and caspase proteolytic activity (Julián, Gandullo, Santos-Silva, Diaz & Martinez, 2013). Legumains are associated with PCD during different steps of plant development (Li et al., 2012; Linnestad et al., 1998); hypersensitive responses (HRs) to pathogens (Rojo et al., 2004) and during compatible interactions between Arabidopsis and various pathogens (Misas-Villamil et al., 2012; Rojo et al., 2004). The pattern of legumain activity observed in this study suggest that this protease could be involved in processing autophagic proteins, although the relationship between these proteases and general or selective autophagy is not fully understood. However, cysteine proteases, especially papain-like cysteine proteases, associated with cytosols and vacuoles, are specifically accumulated in *atg5* mutants (Havé et al., 2018). Caspase 6, which is also involved in the regulation of cell responses to Cd, follows a similar pattern to that of ATG8a protein accumulation. Caspase/metacaspase activity in plants is associated with cell death under different developmental and stress conditions; oxidative stress-induced PCD is an example of a metacaspase-dependent process conserved from protozoa in plants (Fagundes et al., 2015). Metacaspase-dependent autophagy has been described as a *bona fide* mechanism responsible for cell disassembly during vacuolar cell death in Norway spruce embryos (Minina et al., 2013). In tomato cell cultures, although Cd-induced cell death is abolished by caspase inhibitors (Iakimova et al., 2008), the, as yet unidentified, specific link between caspase activity and pexophagy requires further study.

The only well-established relationship between proteases and pexophagy has been reported in relation to peroxisomal LON2 proteases. LON2 proteins are a conserved family of homo-oligomeric ATPases, with both chaperone and protease activities being involved in protein quality control in peroxisomes. Recently, LON2 has been reported to play an important, though ill-defined role, in preventing pexophagy. Expressing protease-deficient, AAA-active LON2 in a *lon2* null mutant prevents pexophagy in *lon2*-deficient mutants, which suggests that the AAA domain of LON2 prevents excessive pexophagy (Goto-Yamada et al., 2014). Further research is required to clarify the contribution of proteases to the regulation of autophagy and pexophagy.

Conclusion

Our findings suggest that pexophagy is crucially involved in rapid cell responses to Cd stress by regulating peroxisomal populations and their quality in order to avoid disturbances in the cell redox balance. This mechanism could involve finely tuned regulation of dynamic changes in peroxisomal populations and peroxisome-dependent signalling events. We also found that NBR1 may be involved in recognizing peroxisomes to be degraded and that peroxisomal H_2O_2 accumulation probably triggers pexophagy through oxidation of an as yet unidentified peroxisomal membrane protein, which acts as an NBR1 cargo receptor. However, given catalase-ATG8 co-localization, in our view, catalase could act as a cargo, although the involvement of other proteins in this process cannot be ruled out. Finally, we show that cathepsin B, legumain and caspase 6 may be involved in the regulation of pexophagy. The scheme in Figure 10, which was adapted from that described by Rodríguez-Serrano et al. (2016), illustrates time course-dependent Cd-induced changes in peroxisomal dynamics beginning with peroxule formation after 30 min of Cd treatment to regulate ROS accumulation and signal transduction followed by further peroxisome proliferation after 3 h of Cd treatment. However, given that peroxisomal homeostasis is highly regulated (Baker & Paudyal, 2014; Reumann & Bartel, 2016) in order to avoid excessive ROS production (Sandalio & Romero-Puertas, 2015), we found that the number of peroxisomes under Cd stress is regulated by pexophagy combined with cathepsin-, legumain- and caspase 6-induced proteolysis. Further study is required to characterize the different peroxisomal receptors and molecular mechanisms involved in protease-regulated pexophagy. Another important issue requiring further in-depth study is the role played by pexophagy in regulating peroxisomal ROS-dependent signal transduction in response to different stress conditions.

References

Álvarez C., García I., Moreno I., Pérez-Pérez M.E., Crespo J.L., Romero L.C. & Gotor C. (2012). Cysteine-generated sulfide in the cytosol negatively regulates autophagy and modulates the transcriptional profile in *Arabidopsis*. *The Plant Cell*, 24(11), 4621-4634.

Avin-Wittenberg T., Baluška F., Bozhkov P.V., Elander P.H., Fernie A.R., Galili G., …, Batoko H. (2018). Autophagy-related approaches for improving nutrient use efficiency and crop yield protection. *Journal of Experimental Botany*, 69(6), 1335-1353.

Baker A. & Paudyal R. (2014). The life of the peroxisome: from birth to death. *Current Opinion in Plant Biology*, 22, 39-47.

Bárány I., Berenguer E., Solís M.T., Pérez-Pérez Y., Santamaría M.E., Crespo J.L., …, Testillano P.S. (2018). Autophagy is activated and involved in cell death with participation of cathepsins during stress-induced microspore embryogenesis in barley. *Journal of Experimental Botany*, 69(6), 1387-1402.

Bánréti A., SassM., Graba Y. (2013) The emerging role of acetylation in the regulation of autophagy. *Autophagy* 9(6), 819–829

Bozhkov P. & Jansson C. (2007). Autophagy and cell-death proteases in plants two wheels of a funeral cart. *Autophagy*, 3(2), 136-138.

Cheng F., Yin L.L., Zhou J., Xia X.J., Shi K., Yu J.Q., …, Foyer C.H. (2016). Interactions between 2-Cys peroxiredoxins and ascorbate in autophagosome formation during the heat stress response in *Solanum lycopersicum*. *Journal of Experimental Botany*, 67(6), 1919-1933.

Chomczynski P. & Sacchi N. (1987). Single-step method of RNA isolation by acid guanidinium thiocyanate-phenol-chloroform extraction. *Analytical Biochemistry*, 162(1), 156-159.

Clemens S (2006) Toxic metal accumulation, responses to exposure and mechanisms of tolerance in plants. *Biochimie* 88(11), 1707-1719

Clemens S. & Ma J.F. (2016). Toxic heavy metal and metalloid accumulation in crop plants and foods. *Annual Review of Plant Biology* 67, 489–512

Costa A., Drago I., Behera S., Zottini M., Pizzo P., Schroeder J.I., …, Lo Schiavo F. (2010). H_2O_2 in plant peroxisomes: an *in vivo* analysis uncovers a Ca^{2+}-dependent scavenging system. *The Plant Journal*, 62(5), 760-772.

Djebali W., Gallusci P., Polge C., Boulila L., Galtier N., Raymond P., …, Brouquisse R. (2008). Modifications in endopeptidase and 20S proteasome expression and activities in cadmium treated tomato (*Solanum lycopersicum* L.) plants. *Planta*, 227(3), 625-639.

Doelling J.H., Walker J.M., Friedman E.M., Thompson A.R. & Vierstra R.D. (2002). The APG8/12-activating enzyme APG7 is required for proper nutrient recycling and senescence in *Arabidopsis thaliana*. *The Journal of Biological Chemistry*, 277(36), 33105–33114.

Fagundes D., Bohn B., Cabreira C., Leipelt F., Dias N., Bodanese-Zanettini M.H. & Cagliari A. (2015). Caspases in plants: metacaspase gene family in plant stress responses. *Functional & Integrative Genomics*, 15(6), 639–649.

Ge Y., Cai Y.M., Bonneau L., Rotari V., Danon A., McKenzie E.A., …, Gallois P. (2016). Inhibition of cathepsin B by caspase-3 inhibitors blocks programmed cell death in *Arabidopsis*. *Cell Death and Differentiation*, 23(9), 1493–1501.

Goto-Yamada S., Mano S., Nakamori C., Kondo M., Yamawaki R., Kato A. & Nishimura M. (2014). Chaperone and protease functions of LON protease 2 modulate the peroxisomal transition and degradation with autophagy. *Plant and Cell Physiology*, 55(3), 482-496.

Grotz N., Guerinot M.L. (2006) Molecular aspects of Cu, Fe and Zn homeostasis in plants. *Biochimica et Biophysica Acta -Molecular Cell Research.*, **1763(7)** , 595 -608

Gupta D.K., Pena L.B., Romero-Puertas M.C., Hernández A., Inouhe M. & Sandalio L.M. (2017). NADPH oxidases differentially regulate ROS metabolism and nutrient uptake under cadmium toxicity. *Plant, Cell and Environment*, 40(4), 509–526.

Havé M., Balliau T., Cottyn-Boitte B., Dérond E., Cueff G., Soulay F., …, Masclaux-Daubresse C. (2018). Increases in activity of proteasome and papain-like cysteine proteases in Arabidopsis autophagy mutants: back-up compensatory effect or cell-death promoting effect? *Journal of Experimental Botany*, 69(6), 1369-1385.

Hofius D., Munch D., Bressendorff S., Mundy J. & Petersen M. (2011). Role of autophagy in disease resistance and hypersensitive response-associated cell death. *Cell Death and Differentiation*, 18(8), 1257–1262.

Hu J. (2010). Molecular basis of peroxisome division and proliferation in plants. *International Review of Cell and Molecular Biology*, 279, 79-99.

Hu J., Baker A., Bartel B., Linka N., Mullen R.T., Reumann S. & Zolman B.K. (2012). Plant peroxisomes: biogenesis and function. *The Plant Cell*, 24(6), 2279–2303.

Julián I., Gandullo J., Santos-Silva L.K., Diaz I. & Martinez M. (2013). Phylogenetically distant barley legumains have a role in both seed and vegetative tissues. *Journal of Experimental Botany*, 64(10), 2929–2941.

Iakimova E.T., Woltering E.J., Kapchina-Toteva V.M., Harren F.J. & Cristescu S.M. (2008). Cadmium toxicity in cultured tomato cells--role of ethylene, proteases and oxidative stress in cell death signaling. *Cell Biology International*, 32(12), 1521-1529.

Kalvari I., Tsompanis S., Mulakkal N.C., Osgood R., Johansen T., Nezis I.P. & Promponas V.J. (2014). iLIR: A web resource for prediction of Atg8-family interacting proteins. *Autophagy*, 10(5), 913-925.

Kellner R., De la Concepcion J.C., Maqbool A., Kamoun S. & Dagdas Y. (2017). ATG8 expansion: a driver of selective autophagy diversification? *Trends in Plant Science*, 22(3), 204-214.

Kim J., Lee H., Lee H.N., Kim S.H., Shin K.D. & Chung T. (2013). Autophagy-related proteins are required for degradation of peroxisomes in *Arabidopsis* hypocotyls during seedling growth. *The Plant Cell*, 25(12), 4956–4966.

Li F. & Vierstra R.D. (2012). Autophagy: a multifaceted intracellular system for bulk and selective recycling. *Trends in Plant Science*, 17(9), 526–537.

Li F., Chung T. & Vierstra R.D. (2014). AUTOPHAGY-RELATED11 plays a critical role in general autophagy- and senescence-induced mitophagy in *Arabidopsis*. *The Plant Cell*, 26(2), 788–807.

Li W.W., Li J. & Bao J.K. (2012). Microautophagy: lesser-known self-eating. *Cellular and Molecular Life Sciences*, 69(7), 1125–1136.

Linnestad C., Doan D.N., Brown R.C., Lemmon B.E., Meyer D.J., Jung R. & Olsen O.A. (1998). Nucellain, a barley homolog of the dicot vacuolar-processing protease, is localized in nucellar cell walls. *Plant Physiology*, 118(4), 1169–1180.

Liu Y. & Bassham D.C. (2012). Autophagy: pathways for self-eating in plant cells. *Annual Review of Plant Biology* 63, 215–237.

Liu Y., Xiong Y. & Bassham D.C. (2009). Autophagy is required for tolerance of drought and salt stress in plants. *Autophagy*, 5(7), 954-963.

Liu Y., Burgos J.S., Deng Y., Srivastava R., Howell S.H. & Bassham D.C. (2012). Degradation of the endoplasmic reticulum by autophagy during endoplasmic reticulum stress in *Arabidopsis. The Plant Cell*, 24(11), 4635–4651.

Liu W., Dai N., Wang Y., Xu C., Zhao H., Xia P., …, Liu Z. (2016). Role of autophagy in cadmium-induced apoptosis of primary rat osteoblasts. *Scientific Reports*, doi: 10.1038/srep20404

Loix C., Huybrechts M., Vangronsveld J., Gielen M., Keunen E., Cuypers A. (2017). Reciprocal interactions between cadmium-induced cell wall responses and oxidative stress in plants. *Frontiers in Plant Science* 8, 1–19

McCarthy I., Romero-Puertas M.C., Palma J.M., Sandalio L.M., Corpas F.J., Gómez M., Del Río L.A (2001) Cadmium induces senescence symptoms in leaf peroxisomes of pea plants. *Plant, Cell and Environment* 24(10), 1065–1073

Masclaux-Daubresse C., Chen Q. & Havé M. (2017). Regulation of nutrient recycling via autophagy. *Current Opinion in Plant Biology*, 39, 8-17.

Michaeli S. & Galili G. (2014). Degradation of organelles or specific organelle components via selective autophagy in plant cells. *International Journal of Molecular Sciences*, 15(5), 7624–7638.

Michaeli S., Galili G., Genschik P., Fernie A.R. & Avin-Wittenberg T. (2016). Autophagy in Plants -- What's New on the Menu? *Trends in plant science*, 21(2), 135-144.

Minina E.A., Filonova L.H., Fukada K., Savenkov E.I., Gogvadze V., …, Bozhkov P.V. (2013). Autophagy and metacaspase determine the mode of cell death in plants. *The Journal of Cell Biology*, 203(6),917-927.

Minina EA, Moschouu PN, Vetukuri RR, Sanchez-Vera V, Cardoso C, …., Bozhkov PV (2018) Transcriptional stimulation of rate-limiting components of the autophagic pathway improves plant fitness. *Journal of Experimental Botany* 69(6) 1415-1432

Misas-Villamil J.C., Toenges G., Kolodziejek I., Sadaghiani A.M., Kaschani F., Colby T., …, van der Hoorn R.A. (2012). Activity profiling of vacuolar processing enzymes reveals a role for VPE during oomycete infection. *The Plant Journal*, 73(4), 689–700.

Mishina N.M., Markvicheva K.N., Fradkov A.F., Zagaynova E.V., Schultz C., Lukyanov S. & Belousov V.V. (2013). Imaging H_2O_2 microdomains in receptor tyrosine kinases signaling. *Methods in Enzymology*, 526, 175-187.

Molins H., Michelet L., Lanquar V., Agorio A., Giraudat J., Roach T., Krieger-Liszkay A., Thomine S. (2013). Mutants impaired in vacuolar metal mobilization identify chloroplasts as a target for cadmium hypersensitivity in *Arabidopsis thaliana*. *Plant Cell Environment*, 36(4), 804-17.

Müntz K. & Shutov A.D. (2002). Legumains and their functions in plants. *Trends in Plant Science*, 7(8), 340-344.

Murashige T. & Skoog F. (1962). A revised medium for rapid growth and bio assays with tobacco tissue cultures. *Physiologia Plantarum*, 15(3), 473–497.

Nelson B.K., Cai X. & Nebenführ A. (2007). A multicolour set of in vivo organelle markers for co-localization studies in *Arabidopsis* and other plants. *The Plant Journal*, 51(6), 1126–1136.

Nevo Y, Nelson N. 2006. The NRAMP family of metal-ion transporters. *Biochimica et Biophysica Acta* 1763(7), 609–620.

Nila A.G., Sandalio L.M., López M.G., Gómez M., del Río L.A. & Gómez-Lim M. (2006). Expression of a peroxisome proliferator-activated receptor gene (x*PPARa*) from *Xenopus laevis* in tobacco (*Nicotiana tabacum*) plants. *Planta*, 224(3), 569–581.

Ohsumi Y. (2014). Historical landmarks of autophagy research. *Cell Research*, 24(1), 9–23.

Oku M. & Sakai Y. (2010). Peroxisomes as dynamic organelles: autophagic degradation. *The FEBS Journal*, 277(16), 3289–3294.

Otsu N. (1979). A threshold selection method from gray-level histograms. *IEEE Transactions on Systems Man and Cybernetics*, 9(1), 62–66.

Paradiso A., Berardino R., de Pinto M.C., Sanità di Toppi L., Storelli M.M., Tommasi F. & De Gara L. (2008). Increase in ascorbate-glutathione metabolism as local and precocious systemic responses induced by cadmium in durum wheat plants. *Plant and Cell Physiology*, 49(3), 362-374.

Pérez-Chaca M.V., Rodríguez-Serrano M., Molina A.S., Pedranzani H.E., Zirulnik F., Sandalio L.M. & Romero-Puertas M.C. (2014). Cadmium induces two waves of reactive oxygen species in *Glycine max* (L.) roots. *Plant, Cell and Environment*, 37(7) 1672–1687.

Pérez-Pérez M.E., Lemaire S.D. & Crespo J.L. (2012). Reactive oxygen species and autophagy in plants and algae. *Plant Physiology*, 160(1), 156–164.

Pfaffl M.W. (2001). A new mathematical model for relative quantification in real-time RT–PCR. *Nucleic Acids Research*, 29(9), e45.

Reumann S. & Bartel B. (2016). Plant peroxisomes: recent discoveries in functional complexity, organelle homeostasis, and morphological dynamics. *Current Opinion in Plant Biology,* 34, 17–26.

Rodríguez-Serrano M., Romero-Puertas M.C., Sparkes I., Hawes C., del Río L.A. & Sandalio L.M. (2009). Peroxisome dynamics in Arabidopsis plants under oxidative stress induced by cadmium. *Free Radical Biology and Medicine*, 47(11), 1632-1639.

Rodríguez-Serrano M., Romero-Puertas M.C., Sanz-Fernández M., Hu J. & Sandalio L.M. (2016). Peroxisomes extend peroxules in a fast response to stress via a reactive

oxygen species-mediated induction of the peroxin PEX11a. *Plant Physiology*, 171(3), 1665–1674.

Rojo E., Martín R., Carter C., Zouhar J., Pan S., Plotnikova J., …, Raikhel N.V. (2014). VPE gamma exhibits a caspase-like activity that contributes to defense against pathogens. *Current Biology*, 14(21), 1897-1906.

Romero-Puertas M.C., Palma J.M., Gómez M., Del Río L.A. & Sandalio L.M. (2002). Cadmium causes the oxidative modification of proteins in pea plants. *Plant, Cell and Environment*, 25(5), 677–686.

Romero-Puertas M.C., Rodríguez-Serrano M., Corpas F.J., Gómez M., del Río L.A. & Sandalio L.M. (2004). Cadmium-induced subcellular accumulation of O_2^- and H_2O_2 in pea leaves. *Plant, Cell and Environment*, 27(9), 1122–1134.

Romero-Puertas M.C., Ortega-Galisteo A.P., Rodríguez-Serrano M. & Sandalio L.M. (2012). Insights into cadmium toxicity: reactive oxygen and nitrogen species function. In *Metal Toxicity in Plants: Perception, Signaling and Remediation* (eds Gupta D.K.G & Sandalio L.M.), pp. 91–117.Springer-Verlag GmbH, Berlin, Heidelberg.

Sandalio L.M., López-Huertas E., Bueno P. & del Río L.A. (1997) Immunocytochemical localization of copper,zinc superoxide dismutase in peroxisomes from watermelon (*Citrullus vulgaris* Schrad.) cotyledons. *Free Radical Research*, 26(3), 187–194.

Sandalio L.M., Dalurzo H.C., Gómez M., Romero-Puertas M.C. & del Río L.A. (2001). Cadmium-induced changes in the growth and oxidative metabolism of pea plants. *Journal of Experimental Botany*, 52(364), 2115–2126.

Sandalio L.M., Rodríguez-Serrano M., Romero-Puertas M.C. & del Río L.A. (2013) Role of peroxisomes as a source of reactive oxygen species (ROS) signaling molecules. *Sub-cellular Biochemistry*, 69, 231–255.

Sandalio L.M. & Romero-Puertas M.C. (2015). Peroxisomes sense and respond to environmental cues by regulating ROS and RNS signalling networks. *Annals of Botany*, 116(4), 475–485.

Shibata M., Oikawa K., Yoshimoto K., Kondo M., Mano S., Yamada K., ..., Nishimura M. (2013). Highly oxidized peroxisomes are selectively degraded via autophagy in *Arabidopsis*. *The Plant Cell*, 25(12), 4967–4983.

Shibata M., Oikawa K., Yoshimoto K., Goto-Yamada S., Mano S., Yamada K., ... , Nishimura, M. (2014). Plant autophagy is responsible for peroxisomal transition and plays an important role in the maintenance of peroxisomal quality. *Autophagy*, 10(5), 936–937.

Sláviková S., Shy G., Yao Y., Glozman R., Levanony H., Pietrokovski S., ..., Galili G. (2005). The autophagy-associated Atg8 gene family operates both under favourable growth conditions and under starvation stresses in Arabidopsis plants. *Journal of Experimental Botany*, 56(421), 2839–2849.

Son Y.O., Wang X., Hitron J.A., Zhang Z., Cheng S., Budhraja A., ...,& Shi X. (2011). Cadmium induces autophagy through ROS-dependent activation of the LKB1-AMPK signaling in skin epidermal cells. *Toxicology and Applied Pharmacology*, 255(3), 287–296.

Svenning S., Lamark T., Krause K., Johansen T. (2011). Plant NBR1 is a selective autophagy substrate and a functional hybrid of the mammalian autophagic adapters NBR1 and p62/SQSTM1. *Autophagy* 7: 993–1010.

Thompson A.R., Doelling J.H., Suttangkakul A. & Vierstra R.D. (2005). Autophagic nutrient recycling in Arabidopsis directed by the ATG8 and ATG12 conjugation pathways. *Plant Physiology*, 138(4), 2097–2110.

Till A., Lakhani R., Burnett S.F. & Subramani S. (2012). Pexophagy: the selective degradation of peroxisomes. International *Journal of Cell Biology*, doi: 10.1155/2012/512721

Van Doorn W.G. & Papini A. (2013). Ultrastructure of autophagy in plant cells: a review. *Autophagy*, 9(12), 1922–1936.

Voitsekhovskaja O.V., Schiermeyer A. & Reumann S. (2014). Plant peroxisomes are degraded by starvation-induced and constitutive autophagy in tobacco BY-2 suspension-cultured cells. *Frontiers in Plant Science*, doi: 10.3389/fpls.2014.00629

Waters, S., K. Marchbank, E. Solomon, C. Whitehouse, and M. Gautel. (2009). Interactions with LC3 and polyubiquitin chains link nbr1 to autophagic protein turnover. *FEBS Lett*. 583:1846–1852.

Woo J., Park E. & Dinesh-Kumar S.P. (2014). Differential processing of Arabidopsis ubiquitin-like Atg8 autophagy proteins by Atg4 cysteine proteases. *Proceedings of the National Academy of Sciences of the United States of America*, 111(2), 863–868.

Xie Q., Michaeli S., Peled-Zehavi H. & Galili G. (2015). Chloroplast degradation: one organelle, multiple degradation pathways. *Trends in Plant Science*, 20(5), 264–265.

Xie Q., Tzfadia O., Levy M., Weithorn E., Peled-Zehavi H., Van Parys T., …, Galili G. (2016). hfAIM: A reliable bioinformatics approach for in silico genome-wide identification of autophagy-associated Atg8-interacting motifs in various organisms. *Autophagy*, 12(5), 876-887.

Yoshimoto K., Hanaoka H., Sato S., Kato T., Tabata S., Noda T. & Ohsumi Y. (2004). Processing of ATG8s, ubiquitin-like proteins, and their deconjugation by ATG4s are essential for plant autophagy. *The Plant Cell*, 16(11), 2967–2983.

Yoshimoto K., Shibata M., Kondo M., Oikawa K., Sato M., Toyooka K., …, Ohsumi Y. (2014) Organ-specific quality control of plant peroxisomes is mediated by autophagy. *Journal of Cell Science*, 127(Pt 6), 1161–1168.

Young P.G. & Bartel B. (2016). Pexophagy and peroxisomal protein turnover in plants. *Biochimica et Biophysica Acta*, 1863(5), 999–1005.

Zhang W. & Chen W. (2011). Role of salicylic acid in alleviating photochemical damage and autophagic cell death induction of cadmium stress in Arabidopsis thaliana. *Photochemical & Photobiological Sciences*, 10(6), 947-955.

Zhang J., Tripathi D.N., Jing J., Alexander, A., Kim, J., Powell, R. T., … Walker, C. L. (2015). ATM functions at the peroxisome to induce pexophagy in response to ROS. *Nature Cell Biology*, 17(10), 1259–1269.

Zhou J., Wang J., Cheng Y., Chi Y.J., Fan B., Yu J.Q. & Chen Z. (2013). NBR1-mediated selective autophagy targets insoluble ubiquitinated protein aggregates in plant stress responses. *PLoS Genetics*, doi: 10.1371/journal.pgen.1003196
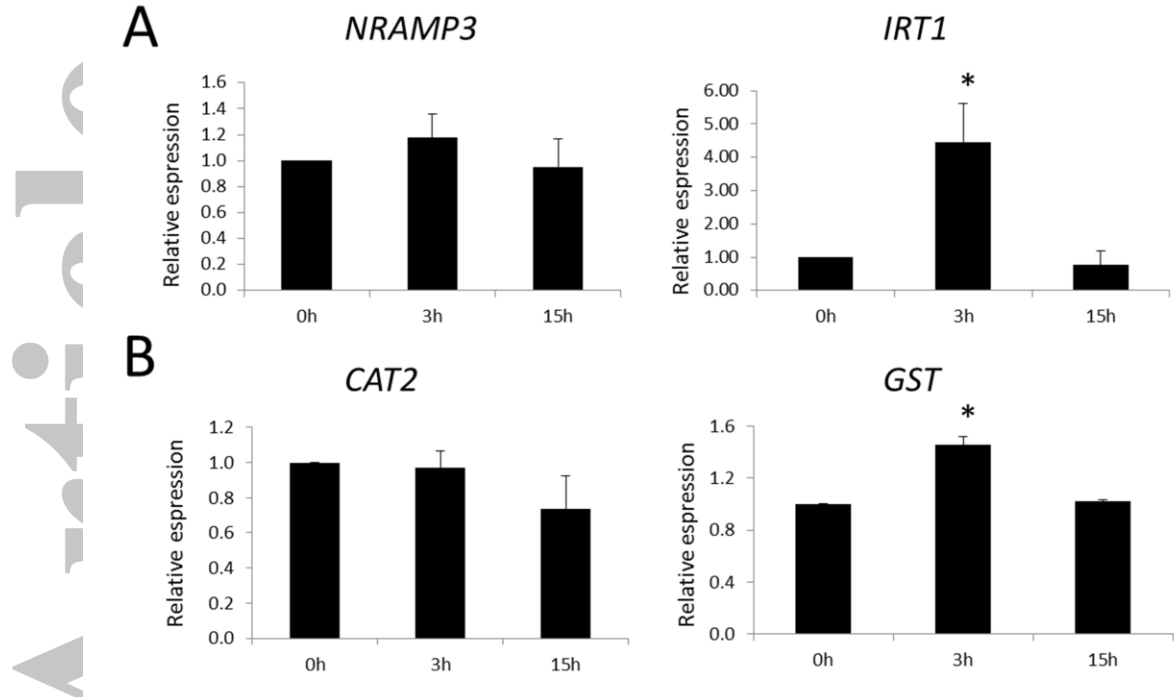
Figure 1. Effect of cadmium on metal transporters and oxidative stress markers. Arabidopsis plants were exposed to 100 µM CdCl$_2$ for 3 and 15 h. Analyses were carried out on whole seedlings. A) Expression of metal transporters *NRAMP3* and *IRT1* genes. B) Expression of antioxidant genes *CAT2* and *GST*. Histograms represent means ±SEM. (*) p <0,05.
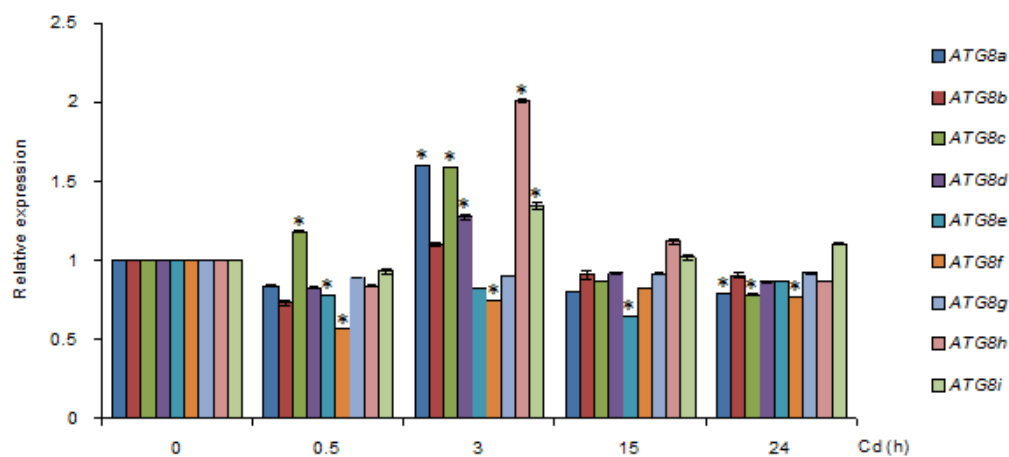
Figure 2. Time course analysis of ATG8 gene family expression in response to treatment with 100 μM CdCl$_2$. Analyses were carried out on whole seedlings. Histograms represent means ±SEM. (*) p < 0,05 (T student test).
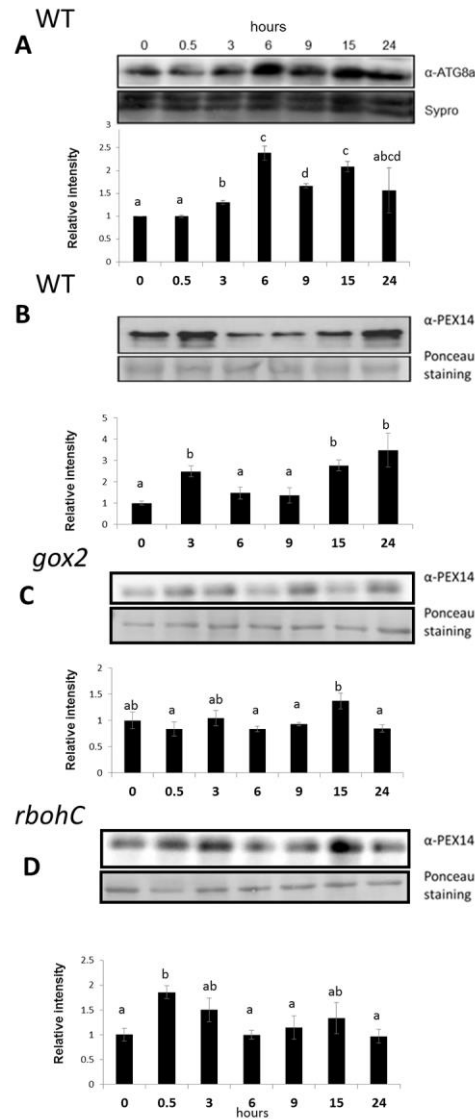
Figure 3. Time course analysis of ATG8a and PEX14 accumulation in Arabidopsis plants treated with 100 µM CdCl$_2$. Analyses were carried out on whole seedlings. A) Representative image of Western blot immunodetection of ATG8a in WT plants. B) Representative image of Western blot immunodetection of PEX14 proteins in WT, C) *gox2* and D) *rboh C* plants. Histograms show protein quantification in each treatment relative to loading control. Value 1 was assigned to the smallest value. The results are representative of three different experiments. Histograms represent means ±SEM. Values followed by different letters are statistically significant. (*) p < 0,05.
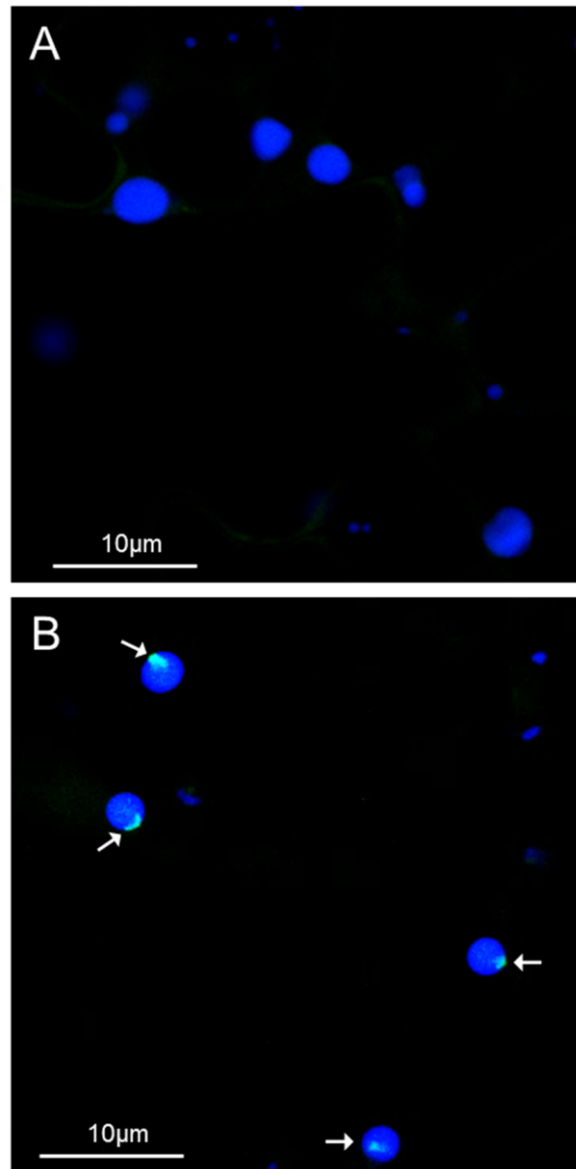
Figure 4. Imaging of pexophagy in Arabidopsis leaves after treatment with 100 μM CdCl$_2$. A) Confocal image of leaves from untreated seedlings and B) seedlings treated with cadmium (6 h) simultaneously expressing GFP-ATG8a (green), as a marker of autophagy, and CFP-SKL (blue) to image peroxisomes. Plants were treated with concanamycin A for 16 h to avoid GFP degradation. Arrows indicate phagophores (green) in contact with peroxisomes (blue).
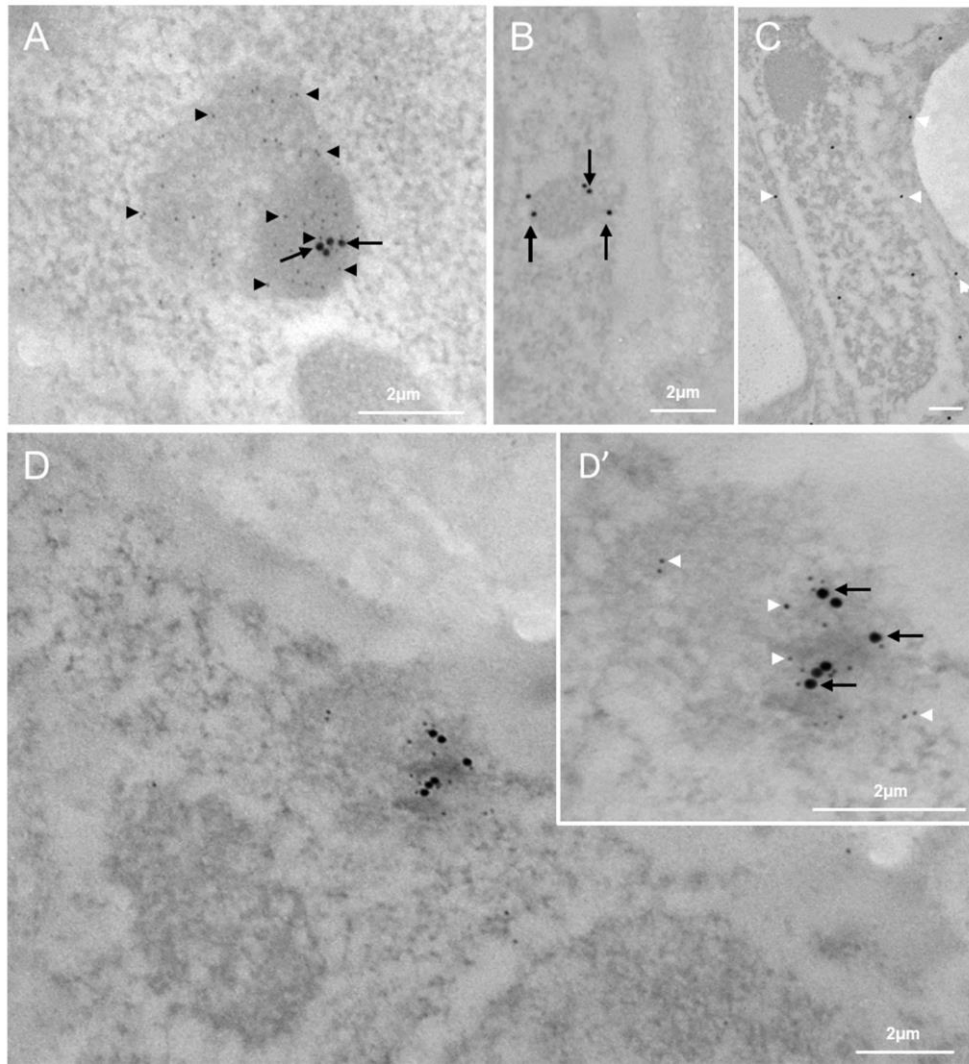
Figure 5. Immunolocalization of potential pexophagy components in Arabidopsis leaves. A) Double immunolocalization of ATG8 (15 nm gold particles) and catalase (5 nm gold particles) using electron microscopy in Arabidopsis leaves from plants treated with Cd for 6 h. Black arrows point to 15 nm gold particles (ATG8a) and black arrowheads point to 5 nm gold particles (catalase). B) ATG8 immunolocalization in electro-lucent vesicles surrounding the electro-dense core of a peroxisome. C) Immunolocalization of NBR1 (white arrowheads, 15 nm gold particles). D) Immunolocalization of ATG8 (15 nm gold particles) and NBR1 (5 nm gold particle) using electron microscopy. D') Magnification of peroxisome observed in previous image. Black arrows point to 15 nm gold particles (ATG8a) and white arrowheads point to 5 nm gold particles (NBR1).
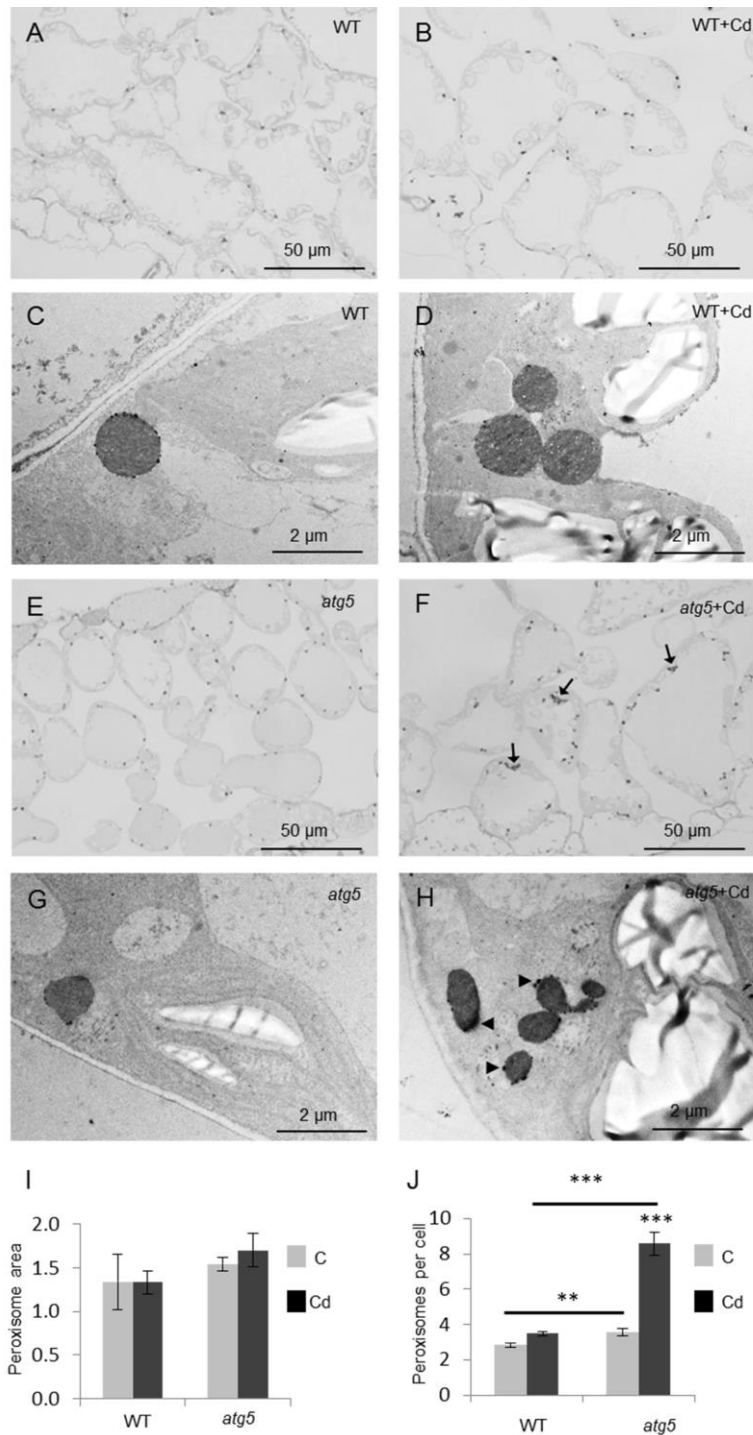
Figure 6. Effect of Cd treatment on peroxisomal distribution in WT and *atg5* Arabidopsis plants. Peroxisomes were imaged by DAB cytochemistry in untreated WT (A and C), Cd-treated WT plants (B and D), in untreated *atg5* plants (E and G) and Cd-treated *atg5* plants (F and H). Arrows in panel F show peroxisome aggregates. Arrowheads in panel H show electro-dense spots inside peroxisomes or close to the peroxisomal membrane. Histograms represent means ±SEM peroxisomal area (I) and number of peroxisomes per cell (J). P< 0.05 (*); P< 0.01 (**); P< 0.001 (***) (T student test).
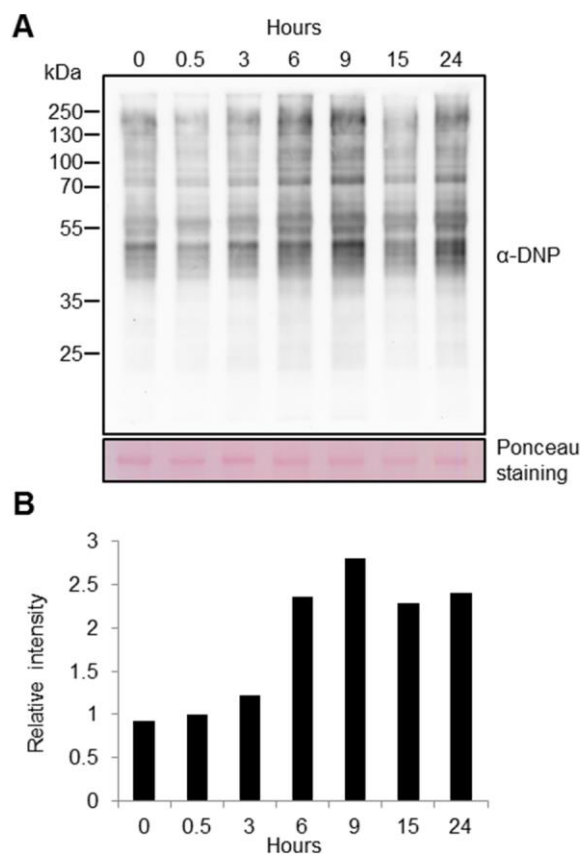
Figure 7. Time course analysis of protein oxidation after treatment with 100 µM CdCl₂. A) Immunochemical detection of carbonylated proteins in cadmium-treated seedlings using anti-DNP antibody. B) Histogram shows total oxidated protein quantification in each treatment relative to loading control. Value 1 was assigned to untreated plants (0 hours). Picture and histograms are representative of two experiments.
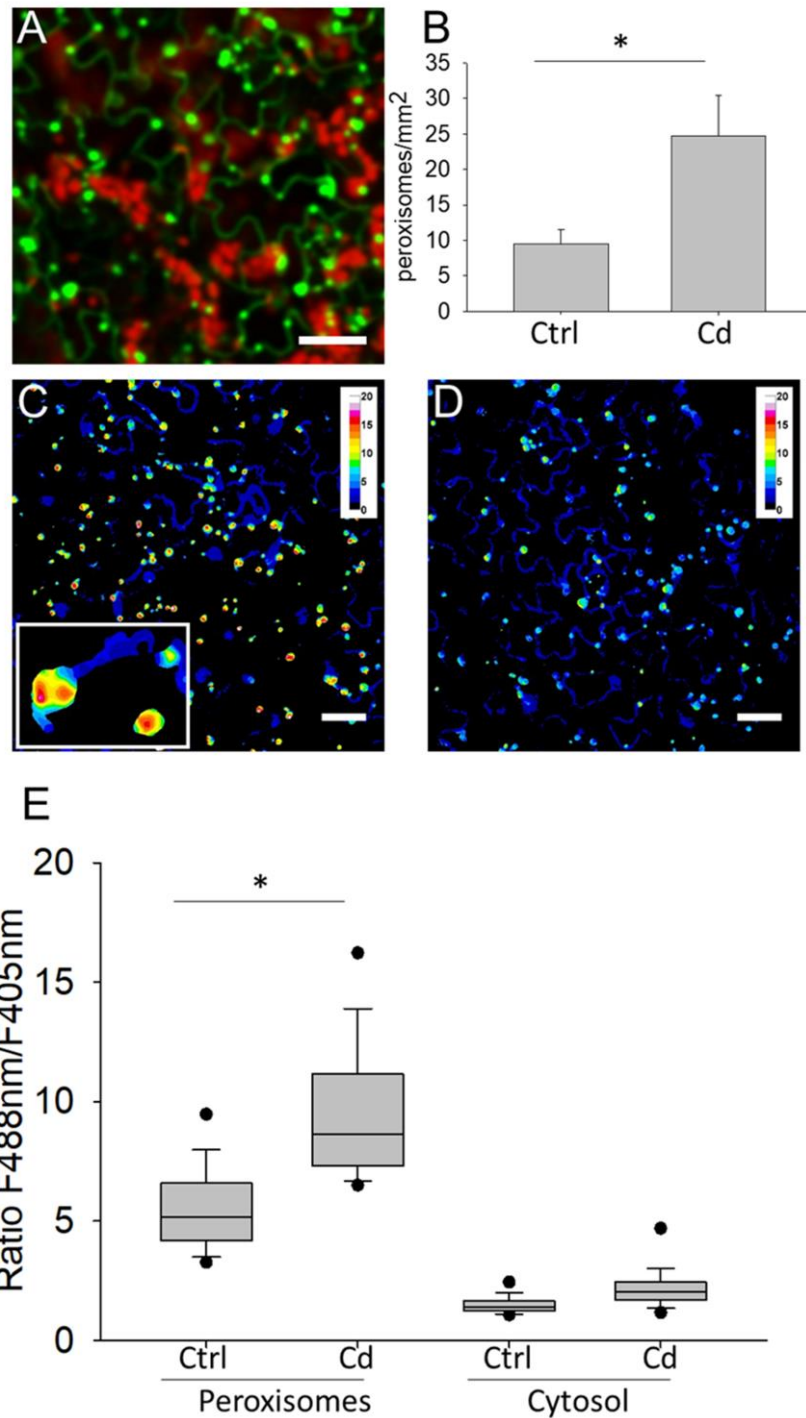
Figure 8. Cd-related redox changes in Arabidopsis peroxisomes. A) HyPer is localized in the peroxisome and cytosol in the stable Arabidopsis line. B) Cd induces peroxisome proliferation after 4 h of Cd treatment. *p = 0.002 (t test). Comparison of 2-week-old Arabidopsis plants treated with Cd (C) and control (D) expressing HyPer in peroxisomes and cytosols shows a significant Cd-related H_2O_2-dependent redox changes in Arabidopsis peroxisomes. Scale bars, 50 µm (all panels). The false color scale applies to all ratio images in the figures. The white rectangle insert shows peroxisomes in detail (enlarged area). Regions of interest (ROIs) of similar size were defined to calculate the HyPer ratio shown in graph (e), n=1059 (Cd) or 390 (ctrl) ROIs in 4-6 images from 2 individual plants. Boxes, lower/upper quartile; whiskers, 5th/95th percentile. (*) p < 0.001 (Dunn's Method).
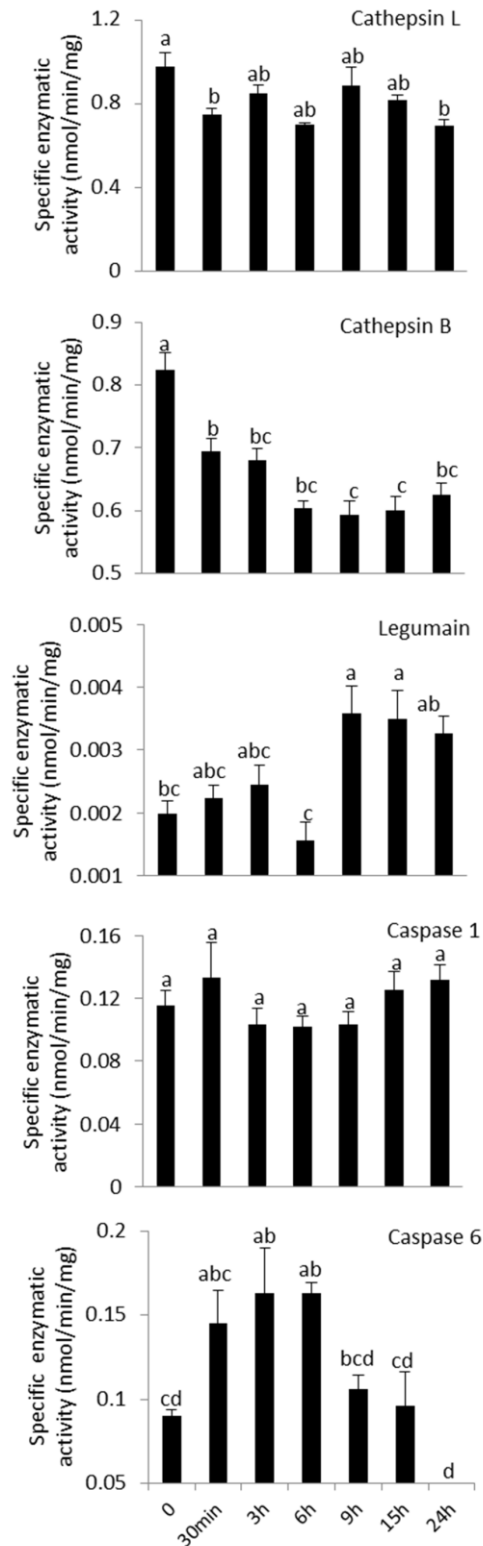
Figure 9. Specific proteolytic activities of cathepsin L- and B-like cysteine protease genes, legumain and caspase 1 and 6 in *A. thaliana* after Cd treatment for 0, 30 min, 3 h, 6 h, 9 h, 15 h and 24 h. Data expressed as nmoles/min/mg are means of 5 replicates ± SEM of duplicate measurements of each sample. Different letters indicate significant differences (one-way ANOVA followed by Tukey´s test; p<0.05).
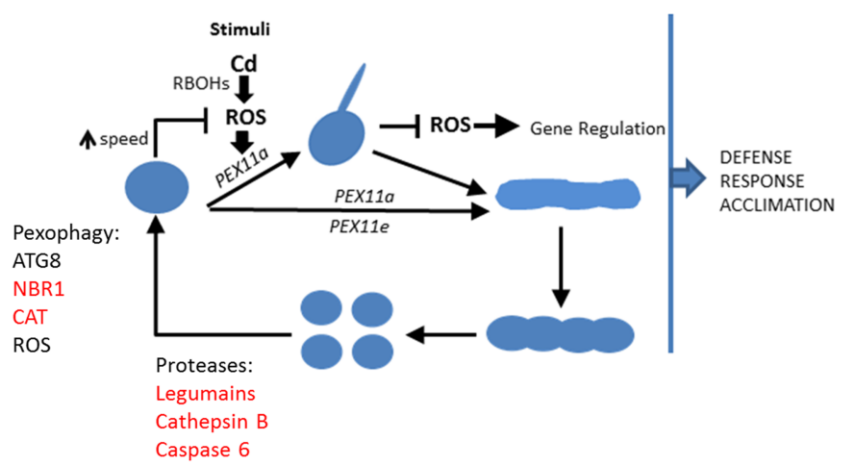
Figure 10. Hypothetical scheme showing changes in peroxisomal dynamics and their regulation in response to Cd treatment (adapted from Rodríguez-Serrano et al., 2016). Cd induces the generation of ROS, which promotes peroxule formation to regulate ROS accumulation and ROS-dependent gene expression. Peroxule formation is followed by elongation, beading and proliferation of peroxisomes. The number of peroxisomes is regulated by pexophagy. Peroxisomes to be degraded could be marked by oxidation of peroxisomal proteins such as catalase, while NBR1 could act as receptor. Legumain, cathepsin B and caspase 6 proteolysis could contribute to the regulation of homeostasis in peroxisomal populations.